Organometallic Complexes of Multianionic Phosphazenates

Gavin T. Lawson,[a] Chacko Jacob,[a] and Alexander Steiner*[a]

Keywords: Phosphazenes / Phosphazenates / Aluminium / Zinc / Multianionic ligands

The amino-substituted phosphazene $P_3N_3(NHCy)_6$ **1** reacts as a multiprotic acid undergoing full deprotonation in the presence of Me_3Al and Et_2Zn, respectively, which results in the formation of multinuclear metal phosphazenates: Trimethyl aluminium deprotonates **1** with evolution of six equivalents of methane to give the pentanuclear organoaluminium complex $[(thfMeAl)(Me_2Al)_4\{P_3N_3(NCy)_6\}]$ **2**. Diethylzinc deprotonates **1** yielding the hexanuclear zinc complex $[(EtZn)_6\{P_3N_3(NCy)_6\}]$ **3**. The higher homologue $P_4N_4(NHCy)_8$ **4** reacts with diethylzinc undergoing sixfold deprotonation giving the hexanuclear complex $[(EtZn)_6\{P_4N_4(NHCy)_2(NCy)_6\}]$ **5**, where two NH functions remain protonated. All three metal complexes **2**, **3** and **5** are soluble in aprotic organic solvents. The highly charged phosphazenate ligands contain three and four PN_4 tetrahedra which are fused in a corner-sharing manner forming P_3N_3 and P_4N_4 ring structures, respectively. These are isoelectronic with *meta*-silicate anions, but in addition equiped with organic groups at terminally arranged N atoms. Both phosphazenate ligands contain various coordination sites and show a high flexibility of their central P–N ring conformation toward the complexed organometallic framework.

Introduction

Metal complexes of multianionic ligand systems (X^{n-}, $n \geq 4$), which are soluble in aprotic organic solvents, are very rare, due to the high polarity of their salt-like structures. Deprotonated calixarenes[1] and porphyrinogens[2] as well as two examples of carbanionic derivatives[3][4] are among the few systems reported so far. Nevertheless, multianionic ligands of high solubility in aprotic organic solvents such as hydrocarbons or aliphatic ethers promise interesting applications in organometallic chemistry, in particular they facilitate multinuclear metal arrangements.

Recently we have shown that cyclic phosphazenes, which are substituted with primary amino groups, can act as multiprotic acids in the presence of strong organometallic bases yielding multianionic phosphazenates, a novel class of highly charged ligand systems (Scheme 1).[5] *n*-Butyllithium deprotonates $P_3N_3\{N(H)Cy\}_6$ (**1**) six times generating the dimeric complex $[(thf)_4Li_{12}\{P_3N_3(NCy)_6\}_2]$ (**1a**).[5a]

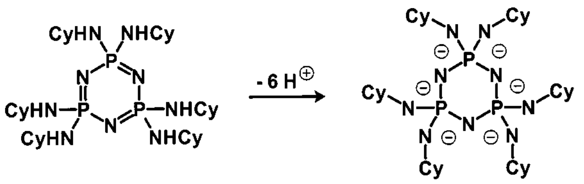

Scheme 1. Multiple deprotonation leading to the phosphazenate hexaanion $[P_3N_3(NCy)_6]^{6-}$

Although **1a** contains two phosphazenate hexaanions $[P_3N_3(NCy)_6]^{6-}$ and twelve lithium cations, it is soluble in hydrocarbons. In fact, $[P_3N_3(NCy)_6]^{6-}$ is the most highly charged anion reported so far, which forms an alkaline metal complex of high solubility in hydrocarbon solvents. Lithium cations are tightly bonded via N atoms to the central P_3N_9 core in **1a**. The peripherally arranged organic groups cover the complex with a lipophilic surface and provide solubility in nonpolar solvents. The central P_3N_3 ring in **1a** is puckered. In contrast, planar ring conformations are usually observed in neutral cyclotriphosphazenes.[6] P−N bond lengths are similar throughout the P_3N_9 core, whereas ring P−N bonds in neutral amino-substituted phosphazenes are usually considerably shorter than P−N bonds involving amino substituents, due to different bond order. Thus it can be assumed that in phosphazenates such as **1a** the negative charge is spread more or less equally over all nitrogen atoms. This is also indicated by the coordination behaviour of $[P_3N_3(NCy)_6]^{6-}$, where all N atoms are involved in coordination to metal centers. Phosphazenate anions are electronically related to silicate anions, which are well-known anionic frameworks in solid-state chemistry. The central P_3N_9 core in $[P_3N_3(NCy)_6]^{6-}$ is isoelectronic to the trimeric *meta*-silicate ion $[Si_3O_9]^{6-}$. In addition it is equiped with organic groups providing solubility in nonpolar media and thus facilitating organometallic chemistry in solution. In particular the generation of multinuclear metal complexes looks very promising due to the number of possible coordination sites and the formally multianionic nature of the ligands. In this paper we present our investigations regarding the coordination behaviour of phosphazenates in multinuclear organometallic complexes of aluminium and zinc.

Results and Discussion

We have treated $P_3N_3(NHCy)_6$ (**1**) with trimethylaluminium or diethylzinc. Both reactions were carried out in refluxing toluene and organometallic reagents were applied

---

[a] Department of Chemistry, University of Liverpool,
Crown Street, Liverpool L69 7ZD, UK
Fax: (internat.) + 44-151/794-3588
E-mail: A.Steiner@liv.ac.uk

in excess (1.2 equiv. per deprotonation step) to ensure high metalation grades. Gas evolution was observed in all cases and clear reaction solutions were obtained. Evaporation of the solvent gave colourless microcrystalline solids, which are thermally stable and show no sign of decomposition below 200°C. However, all obtained metal complexes are air and moisture sensitive and require handling in an inert gas atmosphere.

[(thfMeAl)(Me$_2$Al)$_4${P$_3$N$_3$(NCy)$_6$}] (2)

Complete deprotonation of **1** occurs in the presence of excess Me$_3$Al in toluene. The crude product of the reaction of **1** with Me$_3$Al was crystallised from a mixture of THF/n-hexane. X-ray structure analysis reveals the formation of the pentanuclear aluminium complex [(thfMeAl)(Me$_2$Al)$_4$-{P$_3$N$_3$(NCy)$_6$}] (**2**) (Figure 1).

$$\underset{\mathbf{1}}{P_3N_3(NHCy)_6} + 5\,Me_3Al \rightarrow \underset{\mathbf{2}}{[(thfMeAl)(Me_2Al)_4\{P_3N_3(NCy)_6\}]} + 6\,CH_4 \qquad (1)$$

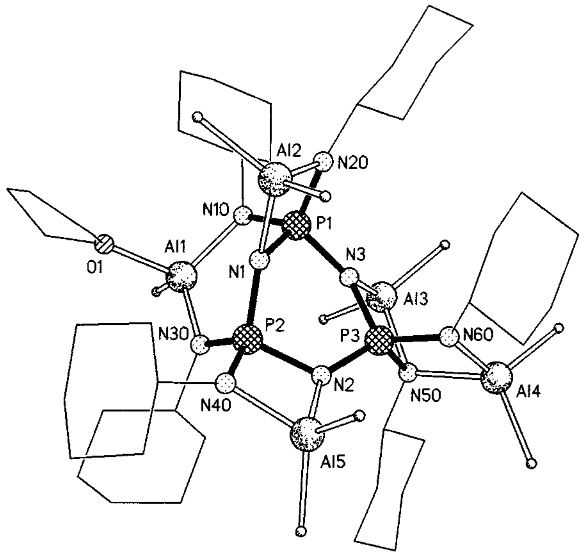

Figure 1. Crystal structure of **2**

Complex **2** contains four Me$_2$Al units and one MeAl unit which is further coordinated by one thf molecule. All five Al atoms have tetrahedral environments and are accommodated in bidentate chelating coordination sites at the centrally arranged phosphazenate core. Al atoms of Me$_2$Al units are coordinated by N−P−N chelates and thus part of four-membered Al−N−P−N ring systems, whereas the aluminium atom of the thfMeAl unit is part of a six-membered Al−N−P−N−P−N ring system. Al−N bond lengths to Me$_2$Al units are slightly longer (av. 1.95 Å) than Al−N lengths to the monomethyl-substituted Al atom (av. 1.86 Å) reflecting the relatively strong Al−N-bonds between the ligand and the formally dicationic MeAl unit. The N−Al−N angle at the AlMe unit is considerably wider [109.4(3)°] than at the Me$_2$Al units [av. 77.0(3)°] (see Table 1). All nitrogen atoms of the phosphazenate core are involved in coordination towards metal centers. Altogether the ligand shows three different coordination pattern in **2**, which are the bidentate chelates **A**, **B** and **C** referring to Scheme 2. Similar coordination pattern have been observed in other aluminium complexes containing P−N ligands, but in contrast to the pentanuclear complex **2**, they exclusively accommodate only one or two metal centers.[7]

Table 1. Selected bond lengths [Å] and angles [°] for **2**

	bond length [Å]		bond length [Å]
P1−N3	1.665(6)	Al1−N10	1.857(6)
P1−N1	1.642(6)	Al1−N30	1.862(7)
P2−N1	1.630(6)	Al1−O1	1.917(6)
P2−N2	1.680(6)	Al2−N20	1.915(7)
P3−N2	1.621(6)	Al2−N1	1.974(6)
P3−N3	1.650(6)	Al3−N3	1.927(6)
P1−N10	1.640(7)	Al3−N50	2.014(7)
P1−N20	1.616(6)	Al4−N60	1.888(6)
P2−N30	1.654(6)	Al4−N50	2.041(7)
P2−N40	1.600(6)	Al5−N40	1.900(6)
P3−N50	1.708(6)	Al5−N2	1.969(6)
P3−N60	1.602(6)		
	bond angle [°]		
N3−P1−N1	106.8(3)		
N1−P2−N2	108.2(3)		
N2−P3−N3	107.5(3)		
N10−P1−N20	118.6(3)		
N30−P2−N40	116.2(3)		
N50−P3−N60	94.8(3)		
P1−N1−P2	116.6(3)		
P2−N2−P3	121.5(4)		
P3−N3−P1	127.0(4)		

The six-membered P−N ring system of the phosphazenate core shows a distorted boat conformation. As already observed in the structure of **1a** there is no marked distinction between terminal and ring P−N-bond lengths in **2** (see Table 1), with the exception of the rather long bond between P-3 and N-50 which is coordinating to two aluminium atoms. The P−N-stretching frequency of the phosphazenate ring in **2** (1079 cm^{-1}) is red-shifted compared to corresponding bands in IR spectra of neutral amino-substituted phosphazenes (1200 cm^{-1})[6] indicating a decrease in bond order between ring atoms from the neutral to the metalated species as well as strong interactions between metal centers and ligand N atoms.

Three signals are present in the ^{31}P NMR spectrum of **2** due to the three nonequivalent phosphorus atoms, thus dynamic behaviour at room temperature can be excluded. As expected each ^{31}P signal shows a dd pattern. However coupling constants differ markedly between ^{31}P nuclei. Whereas two coupling constants are relatively large (J = 12.4 and 16.3 Hz, respectively), the third one amounts only to 2.5 Hz, indicating low electronic interactions across one P−N−P unit within the P$_3$N$_3$ ring. The ^{1}H spectrum of **2** is rather complex, due to nonequivalent substituents. Me$_2$Al protons appear between $\delta = -0.1$ and $-\delta = 0.4$, whereas the protons of the MeAl unit show a chemical shift of $\delta = 0.61$.

[(EtZn)$_6${P$_3$N$_3$(NCy)$_6$}] (3)

Treatment of **1** with excess Et$_2$Zn in toluene leads to complete deprotonation of the hexaprotic phosphazene precursor, which results in the formation of the hexanuclear zinc complex $[(EtZn)_6\{P_3N_3(NCy)_6\}]$ (**3**) (Figure 2).

$$\underset{\mathbf{1}}{P_3N_3(NHCy)_6} + 6\,Et_2Zn \rightarrow \underset{\mathbf{3}}{[(EtZn)_6\{P_3N_3(NCy)_6\}]} + 6\,C_2H_6 \quad (2)$$

Six metal atoms occupy bi- and tridentate coordination sites in **3** encapsulating the centrally arranged multidentate ligand. Four ethylzinc moieties are accommodated in tripodal sites, two of type **D** (Zn-2, Zn-3) and two of type **E** (Zn-1, Zn-4), resulting in a cage structure comprising the phosphazenate ring atoms, the four terminal N atoms N-10, N-20, N-40, N-60 and the aforementioned four Zn atoms. The other two ethylzinc units (Zn-5, Zn-6) are chelated in the bidentate fashion **B**. All nitrogen functions are involved in coordination toward metal atoms. Zn−N distances vary widely and depend mainly on coordination numbers of participating atoms. These correspond to those found in zinc phosphazene complexes containing related coordination sites.[8] The shortest distances are observed between the tri-coordinate zinc atoms and the terminally arranged N atoms [av. 1.90 Å]. Distances of Zn-5 and Zn-6 to the ring−N-functions are considerably longer [av. 2.31 Å]. Within tripodal sites of the cage each zinc atom has two shorter [av. 2.12 Å] and one longer Zn−N-bond [av. 2.43 Å]. An interesting feature of **3** is the substantial involvement of N_{ring} atoms in coordination toward metal centers. Each one interacts with two zinc atoms, resulting in a distorted tetrahedral environment at N-2 (av. Zn−N−Zn 99°) and in an almost linear Zn−N−Zn arrangement at N1 and N3 (av. 157°). P−N lengths of ring- and terminally located P−N-bonds in **3** are in the same range [av. 1.64 Å] indicating equal charge distribution over all N-functions (see Table 2). The six-membered phosphazenate ring system in **3** adopts a *twist* conformation.

NMR-spectra of **3** are in correspondence with the crystal structure (Table 4). ^{31}P NMR of **3** shows a triplet (P-1) and a doublet (P-2/P-3) in the intensity ratio 1:2 reflecting the molecular C_2-symmetry of **3**, where P-1 and N-2 are located on a noncrystallographic C_2-axis. The ^{1}H NMR shows two distinct environments for zinc-bonded ethyl groups, which can be assigned to bidentate and tripodal coordination sites, respectively. The very strong P−N-stretch band appears at 1055 cm^{-1} and is, as in **2**, markedly red-shifted compared to corresponding bands of neutral phosphazenes.

Coordination Pattern of the Hexaanionic Ligand System $[P_3N_3(NCy)_6]^{6-}$

Scheme 2 illustrates the coordination modes which we have observed so far in complexes containing the hexaanionic ligand system $[P_3N_3(NCy)_6]^{6-}$. Both terminal and ring N atoms can take part in coordination to metal centers via bidentate (**A**, **B** and **C**) as well tripodal sites (**D**, **E** and **F**). Exclusively bidentate coordination sites of type **A**, **B** and **C** are present in the aluminium complex **2**, resulting in four (**A** and **B**) and six-membered (**C**) metallo heterocycles. Ethylzinc moieties in **3**, occupy in addition to the bidentate site **B**, tripodal sites of type **D** and **E**. Another tripodal coordination mode, which involves exclusively terminal N atoms of one ligand face resulting in a hetero-adamantane cage (**F**), has been observed in the lithium complex **1a**.[5a]

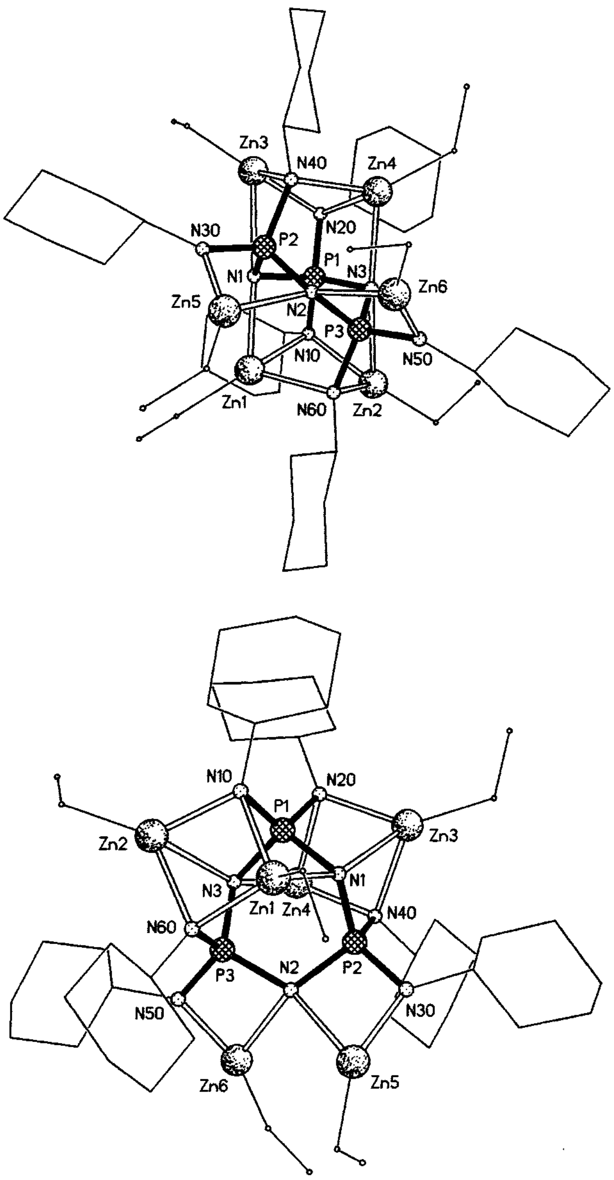

Figure 2. Crystal structure of **3** showing two views from different angles. Only one of two independent complexes in the asymmetric is shown

Six-membered phosphazenate ring systems in **2** and **3** are puckered as in the lithium complex **1a**, which is in contrast to the usually planar arrangement of six-membered rings in neutral cyclotriphosphazenes.[6] This reflects the high flexibility of the phosphazenate backbone in the presence of cooordinated metal centers. The complexed metal array determines the conformation of the central P_3N_3 ring, resulting in a *chair* conformation in the presence of lithium cations in **1a**, a *boat* conformation in the organo aluminium complex **2** and a *twist* conformation in the organozinc derivative **3**.

Table 2. Selected bond lengths [Å] and angles [°] for **3**

	bond length [Å]			bond length [Å]	
P1−N3	1.664(12)	1.661(13)	Zn1−N1	2.157(12)	2.190(11)
P1−N1	1.677(12)	1.663(12)	Zn1−N10	2.307(12)	2.314(12)
P2−N1	1.651(13)	1.648(12)	Zn1−N60	2.160(12)	2.105(12)
P2−N2	1.662(12)	1.678(13)	Zn2−N3	2.548(12)	2.433(13)
P3−N2	1.671(12)	1.670(13)	Zn2−N10	2.026(12)	2.028(12)
P3−N3	1.622(12)	1.647(13)	Zn2−N60	2.147(12)	2.148(12)
P1−N10	1.625(12)	1.631(13)	Zn3−N1	2.531(12)	2.480(11)
P1−N20	1.616(13)	1.617(13)	Zn3−N20	2.012(13)	2.042(12)
P2−N30	1.619(12)	1.612(13)	Zn3−N40	2.128(12)	2.147(11)
P2−N40	1.647(12)	1.664(12)	Zn4−N3	2.201(12)	2.220(13)
P3−N50	1.637(12)	1.587(13)	Zn4−N20	2.358(13)	2.318(12)
P3−N60	1.650(12)	1.672(13)	Zn4−N40	2.110(12)	2.126(11)
			Zn5−N2	2.313(12)	2.293(13)
			Zn5−N30	1.889(12)	1.904(12)
			Zn6−N2	2.313(12)	2.245(13)
			Zn6−N50	1.885(12)	1.903(13)

	bond angle [°]	
N3−P1−N1	105.8(6)	106.7(6)
N1−P2−N2	110.2(6)	109.6(6)
N2−P3−N3	108.8(6)	107.8(6)
N10−P1−N20	122.7(7)	122.1(7)
N30−P2−N40	116.3(6)	117.3(6)
N50−P3−N60	114.1(7)	116.8(6)
P1−N1−P2	114.3(7)	115.7(7)
P2−N2−P3	112.6(7)	114.3(8)
P3−N3−P1	116.5(7)	116.6(8)

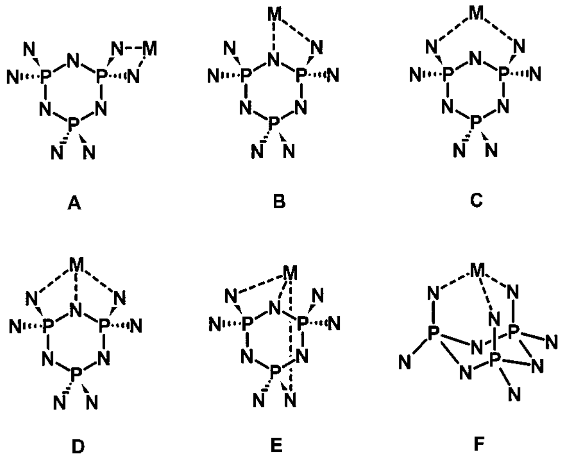

Scheme 2. Coordination pattern of the hexaanionic ligand system $[P_3N_3(NCy)_6]^{6-}$

$[(EtZn)_6\{P_4N_4(N(H)Cy)_2(NCy)_6\}]$ (5)

Having studied the coordination behaviour of the six-membered ring phosphazenate $[P_3N_3(NCy)_6]^{6-}$ in the presence of various metal environments we were interested what type of coordination modes its higher homologue $[P_4N_4(NCy)_8]^{8-}$ might adopt. So far we have succeeded in determining the structure of the product gained from the reaction of $P_4N_4(NHCy)_8$ (**4**) with diethylzinc: Although an excess of Et_2Zn has been used only six of the eight NH functions in **4** have been deprotonated, even after refluxing the reaction mixture for 12 h in toluene. The hexanuclear zinc complex **5** has been isolated which contains the hexaanionic ligand system $[P_4N_4(NHCy)_2(NCy)_6]^{6-}$ (Figure 3)

$$\underset{\mathbf{4}}{P_4N_4(NHCy)_8} + 6\,Et_2Zn \rightarrow \underset{\mathbf{5}}{[(EtZn)_6\{P_4N_4(NHCy)_2(NCy_6\}]} + 6\,C_2H_6 \quad (3)$$

The structure of **5** is closely related to that of **3**: The six zinc atoms occupy bi- and tridentate coordination sites around the centrally arranged multidentate ligand. Four EtZn units are accommodated in tripodal sites (Zn-1, Zn-2, Zn-3 and Zn-4), resulting in cage structure assembled of phosphazenate ring atoms, four terminal N-functions and the four Zn atoms. Zn-5 and Zn-6 are chelated in bidentate ligand sites. The complex exhibits noncrystallographic C_2-symmetry. Structural parameters involving metal centers correspond largely to those observed in **3** (see Table 3) and coordination modes around the P_4N_{12} core of **5** resemble types **B**, **D** and **E** of the P_3N_9 core (Scheme 2). It is worth mentioning that both complexes **3** and **5** are the only ones which have been structurally characterised so far, where one single ligand accommodates such a large number of Zn atoms.

Two N functions in **5** remain protonated, even if excess of the strong organozinc base is used. This is also indicated by the appearance of a weak N−H-band at 3400cm^{-1} in the IR spectrum of **5**. The incomplete deprotonation of **4** in the presence of Et_2Zn can be rationalised by the increased number of sterically demanding cyclohexyl groups covering the surface of the complexes (from six in **3** to eight in **5**), which is accompanied by only modest expansion of the ligand core. With the exception of the two protonated N atoms, all nitrogen-functions are involved in coordination toward metal-centers. The P_4N_4 ring is puckered and has a similar conformation to that in the tetraanionic ligand system $[N_4\{P(Ph)(NCy)\}_4]^{4-}$.[5b]

Two signals in the ^{31}P NMR of **5** reveal two pairs of chemically equivalent phosphorus nuclei: P-1 and P-3 are carrying exclusively deprotonated substituents, whereas both P-2 and P-4 are bonded to one deprotonated and one protonated nitrogen atom. Surprisingly both ^{31}P NMR signals in **5** exist of doublets, where one would anticipate a set of two triplets in case the four ^{31}P nuclei act as a A_2B_2-system. Temperature dependent measurements (−80°C to 40°C) indicate no sign of fluctuation within the complexes. The $^3J_{P-P}$ coupling constants across two P−N−P units located opposite to each other in the P_4N_4 ring might be too small to be observed. A similar observation was made in **2**, where one P−N−P unit gave a considerably lower coupling constant as the other two P−N−P units. The ^1H NMR spectrum resembles that of **3**. There are two distinct sets of signals for zinc-bonded ethyl groups, which can be assigned to tripodal and bidentate coordination sites, respectively. However, evidence for both protonated NH groups cannot be drawn from the ^1H NMR spectrum, due to overlap of the NH-signal with the complex pattern of cyclohexyl groups.

Conclusion

Organometallic complexes of multianionic phosphazenates have been generated by deprotonation reactions of

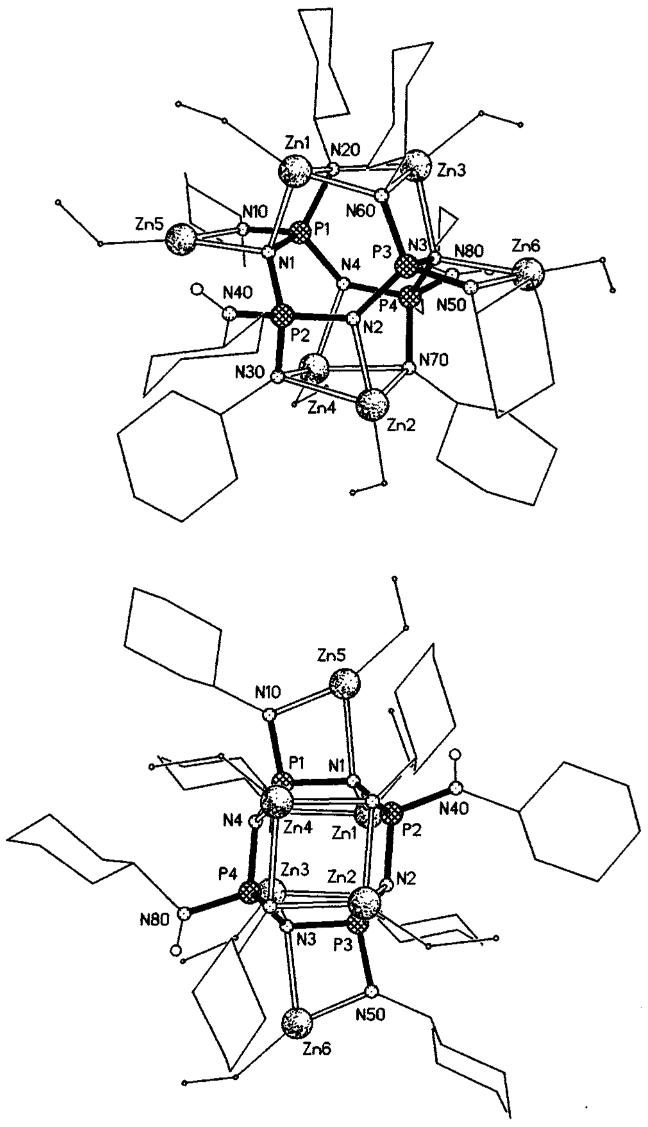

Figure 3. Crystal structure of **5** showing two views from different angles

amino-substituted phosphazenes with strong organometallic bases. The high charge of these new ligands facilitates the accommodation of a large number of metal cations per ligand molecule. The lipophilic character of these systems provides synthetic applications in aprotic organic solvents. We are focussing on transition metal complexes and extending our investigations to polymeric derivatives based on polyphosphazenates. Metal complexes of polyphosphazenates promise novel hybrid materials with unusual electronic or magnetic properties depending on the accommodated metal species. The organic substituent determines the appearance and flexibility of the material (e.g. films, fibres, glasses). Small molecular derivatives, such as the cyclic phosphazenates presented in this paper, can act as useful model compounds mimicking the microscopic behaviour of the corresponding polymer.

Table 3. Selected bond lengths [Å] and angles [°] for **5**

	bond length [Å]		bond length [Å]
P1−N1	1.670(11)	Zn1−N1	2.132(11)
P1−N4	1.613(11)	Zn1−N20	2.319(12)
P1−N10	1.626(9)	Zn1−N60	2.001(10)
P1−N20	1.646(11)	Zn2−N3	2.138(11)
P2−N1	1.644(11)	Zn2−N20	2.025(11)
P2−N2	1.617(10)	Zn2−N60	2.363(11)
P2−N30	1.642(11)	Zn3−N2	2.098(11)
P2−N40	1.609(13)	Zn3−N30	2.314(10)
P3−N2	1.626(11)	Zn3−N70	2.101(13)
P3−N3	1.660(11)	Zn4−N4	2.132(13)
P3−N50	1.611(9)	Zn4−N30	2.085(13)
P3−N60	1.648(10)	Zn4−N70	2.252(11)
P4−N3	1.639(11)	Zn5−N1	2.272(9)
P4−N4	1.635(10)	Zn5−N10	1.888(11)
P4−N70	1.639(11)	Zn6−N3	2.276(10)
P4−N80	1.623(13)	Zn6−N50	1.888(10)

	bond angle[°]
N4−P1−N1	110.2(6)
N10−P1−N20	115.2(6)
N2−P2−N1	114.4(6)
N40−P2−N30	113.7(7)
N2−P3−N3	107.9(6)
N50−P3−N60	116.4(5)
N4−P4−N3	111.9(5)
N80−P4−N70	112.4(7)
P1−N1−P2	122.4(6)
P2−N2−P3	129.4(7)
P3−N3−P4	124.4(7)
P1−N4−P4	130.8(7)

Experimental Section

General Remarks: All manipulations were performed under dry nitrogen atmosphere in standard Schlenk-glassware or in a glove box. − Solvents were dried over sodium (toluene) and potassium (hexane, THF), respectively. − Precursors **1** and **4** were prepared according to literature methods.[9] Organometallic reagents were applied as standard solutions: Me_3Al, 2.0 M in hexane (Aldrich); Et_2Zn, 1.0 M in hexane (Aldrich). − FT-IR spectra were recorded on a Perkin−Elmer Paragon 1000 spectrometer in nujol between CsI plates. − NMR spectra were recorded on a Bruker AMX 400 spectrometer.

Preparation of [(thfMeAl)(Me₂Al)₄{P₃N₃(NCy)₆}] (2): Me_3Al (5 mL of a 2.0 M solution in hexane, 10 mmol) was added to a solution of **1** (1 g, 1.38 mmol) in toluene (20 mL). The reaction mixture was refluxed for 1 h, then stirred for 30 min at room temperature and subsequently filtered through Celite. The solvent was evaporated and the residue recrystallised from of THF/hexane solution. After storage at room temperature for several days, colourless crystals of the solvate **2**·THF·hexane were obtained. Lattice solvent could be removed in vacuum. Yield of lattice solvent free product: 1.07 g, 1.01 mmol (73%). − ^1H NMR (400 MHz, $CDCl_3$, 25°C, TMS): δ = −0.4 to −0.1 [b, 24 H, $(CH_3)_2Al$], 0.61 (b, 3 H, CH_3Al), 1.40 (m, 4 H, thf), 1.5−2.4 [m, 60 H, $CH(CH_2)_5$], 2.56 (m, 4 H, thf), 3.42 [m, 6 H, $CH(CH_2)_5$]. − ^{31}P NMR (162 MHz, $CDCl_3$, 25°C, 85% H_3PO_4): δ = 9.55 (dd, $^2J_{P-P}$ = 2.5, 16.3 Hz), 12.5 (dd, $^2J_{P-P}$ = 12.4, 16.3 Hz), 16.4 (dd, $^2J_{P-P}$ = 2.5, 12.4 Hz). − IR (Nujol): $\tilde{\nu}$ [cm^{-1}] = 1413, 1293, 1260, 1216, 1190, 1124, 1079 (vs, P−N stretch), 1029, 956, 890. 849, 816, 630. − $C_{49}H_{101}Al_5N_9OP_3$ (1060.23): calcd. C 55.51, H 9.60, N 11.89; found C 54.89, H 9.51, N 11.64.

Preparation of [(EtZn)₆{P₃N₃(NCy)₆}] (3): Et_2Zn (10 mL of a 1.0 M solution in hexane, 10 mmol) was added to a solution of **1** (1 g, 1.38 mmol) in toluene (20 mL). The reaction mixture was refluxed

Table 4. Crystal data of **2**, **3** and **5**

	2 × THF × hexane	**3**	**5** × hexane
Empirical formula	$C_{59}H_{123}Al_5N_9O_2P_3$	$C_{48}H_{96}N_9P_3Zn_6$	$C_{66}H_{134}N_{12}P_4Zn_6$
Molecular mass	1218.47	1284.47	1611.95
a [Å]	13.082(4)	21.919(12)	12.681(6)
b [Å]	23.821(4)	22.085(6)	14.858(6)
c [Å]	23.327(3)	13.544(5)	22.153(8)
α [°]	90	99.90(3)	86.64(7)
β [°]	98.30(2)	105.27(5)	82.71(6)
γ [°]	90	102.44(4)	69.43(6)
V [Å^3]	7139(3)	5992(4)	3876(3)
Crystal system	Monoclinic	Triclinic	Triclinic
Space group	$P2_1/n$	P1bar	P1bar
Crystal size [mm^3]	0.25 × 0.25 × 0.20	0.30 × 0.30 × 0.25	0.40 × 0.35 × 0.15
Z	4	4	2
ρ_{calc} [g cm^{-3}]	1.125	1.424	1.381
μ (Mo-K_α) [mm^{-1}]	0.187	2.482	1.955
F(000)	2664	2688	1708
Transmission$_{max/min}$	1.000/0.932	0.967/0.562	0.988/0.549
Refl. collected	9738	16175	10586
Refl. unique (R_{int})	9344 (0.063)	15690 (0.074)	10125 (0.078)
Data/parameter	9344/703	15690/645	10125/709
$R1$ [$I > 2\sigma(I)$]	0.089 (6618 refl.)	0.081 (8517 refl.)	0.096 (5167 refl.)
$WR2$ (all data)	0.258	0.223	0.287
Final diff map [eÅ^{-3}]	0.62/−0.61	1.13/−1.10	1.23/−1.33

for 1 h, then stirred for 30 min at room temperature and subsequently filtered through Celite. The solvent was evaporated and the residue recrystallised from of THF/hexane solution. After storage at room temperature for several days, colourless crystals of **3** were obtained. Yield: 1.17 g, 0.91 mmol (66%). − ^{1}H NMR (400 MHz, $CDCl_3$, 25°C, TMS): δ = 0.25 (q, 4 H, $CH_3C\mathit{H}_2Zn$), 0.34 (q, 8H $CH_3C\mathit{H}_2Zn$), 0.91 (t, 6 H, $C\mathit{H}_3CH_2Zn$), 1.10 (t, 12 H, $C\mathit{H}_3CH_2Zn$), 1.1−2.2 [m, 60 H, $CH(C\mathit{H}_2)_5$], 2.97 [m, 6 H, $C\mathit{H}(CH_2)_5$]. − ^{31}P NMR (162 MHz, $CDCl_3$, 25°C, 85% H_3PO_4): δ = 31.2 (d, $^2J_{P-P}$ = 11 Hz), 33.5 (t, $^2J_{P-P}$ = 11 Hz). − IR (Nujol): $\tilde{\nu}$ [cm^{-1}] = 1409, 1290, 1261, 1229, 1200, 1145, 1079, 1055 (vs, P−N stretch), 1023, 994, 944, 886, 846, 804, 609. − $C_{48}H_{96}N_9P_3Zn_6$ (1284.47): calcd. C 44.88, H 7.53, N 9.81; found C 44.54, H 7.44, N 9.58.

Preparation of $[(EtZn)_6\{P_4N_4(N(H)Cy)_2(NCy)_6\}]$ (5): Et_2Zn (10 mL of a 1.0 M solution in hexane, 10 mmol) was added to a solution of **4** (1 g, 1.04 mmol) in toluene (20 mL). The reaction mixture was refluxed for 1 h, then stirred for 30 min at room temperature and subsequently filtered through Celite. The solvent was evaporated and the residue recrystallised from of thf/hexane solution. After storage at room temperature for several days, colourless crystals of the solvate **5**·hexane were obtained. Lattice solvent could be removed in vacuum. Yield of solvent free product: 0.84 g, 0.55 mmol (53%). − ^{1}H NMR (400 MHz, $CDCl_3$, 25°C, TMS): δ = 0.21 (q, 4 H, $CH_3C\mathit{H}_2Zn$), 0.28 (q, 8 H, $CH_3C\mathit{H}_2Zn$), 0.50 (t, 6 H, $C\mathit{H}_3CH_2Zn$), 0.93 (t, 12 H, $C\mathit{H}_3CH_2Zn$), 1.1−2.2 [m, 80 H, $CH(C\mathit{H}_2)_5$], 3.04 [m, 8 H, $C\mathit{H}(CH_2)_5$]. − ^{31}P NMR (162 MHz, $CDCl_3$, 25°C, 85% H_3PO_4): δ = 21.3 (d, $^2J_{P-P}$ = 10 Hz), 26.4 (d, $^2J_{P-P}$ = 10 Hz). − IR (Nujol): $\tilde{\nu}$ [cm^{-1}] = 3400 (w, N−H stretch), 1579, 1261, 1071 (vs, P−N stretch), 1021, 930, 887, 798, 666; $C_{60}H_{120}N_{12}P_4Zn_6$ (1525.87): calcd. C 47.23, H 7.93, N 11.02; found C 46.84, H 7.94, N 10.78.

X-ray Structure Determination of 2, 3 and 5: Crystal data were recorded on a Rigaku-AFC6S diffractometer, Mo-K_α radiation (λ = 0.71073 Å), T = 153 K, $2\theta_{max.}$ = 45°, $2\theta/\omega$-scan mode, absorption corrections based on ψ-scans, structures were solved by direct methods and refined by full-matrix least squares against F^2 using all data.[10] The asymmetric unit of the crystal structure of **3** contains two crystallographically independent complexes. Crystals of **2** and **5** crystallise as solvates: Asymmetric unit content: **2**·THF·hexane, **3** and **5**·hexane, respectively. Lattice solvents in both structures are disordered as well as part of ethyl groups in **3** and **5** and cyclohexyl groups in **5**. Disordered groups were split on two positions and refined using geometrical restraints. All nonhydrogen groups were refined anisotropically with the exception of lattice solvent molecules, C and N positions in **3** and disordered C positions in **5**, which were refined isotropically. H positions were fixed geometrically. Crystallographic data (excluding structure factors) for the structures reported in this paper have been deposited with the Cambridge Crystallographic Data Centre as supplementary publications no. CCDC-118485 (**2**), CCDC-118486 (**3**) and CCDC-118487 (**5**). Copies of the data can be obtained free of charge on application to CCDC, 12 Union Road, Cambridge CB2 1EZ, UK (Fax: (internat.) + 44-1223/336−033; E-mail: deposit@ccdc.cam.ac.uk

Acknowledgments

This work was supported by the EPSRC, the Royal Society, the Nuffield Foundation and the Research Development Fund, University of Liverpool.

---

[1] J. M. Smith, S. G. Bott, *Chem. Commun.* **1996**, 377.

[2] [2a] S. De Angelis, E. Solari, C. Floriani, A. Chiesi-Villa, C. Rizzoli, *J. Chem. Soc., Dalton Trans.* **1994**, 2467. − [2b] C. Floriani, *Chem. Commun.* **1996**, 1257.

[3] M. Winkler, M. Lutz, G. Müller, *Angew. Chem. Int. Ed. Engl.* **1994**, *33*, 2279.

[4] H. Bock, K. Gharagozloo-Hubmann, C. Näther, N. Nagel, Z. Havlas, *Angew. Chem. Int. Ed. Engl.* **1996**, *35*, 631.

[5] [5a] A. Steiner, D. S. Wright, *Angew. Chem. Int. Ed. Engl.* **1996**, *35*, 636. − [5b] A. Steiner, D. S. Wright, *Chem. Commun.* **1997**, 283.

[6] [6a] H. R. Allcock, *Chem. Rev.* **1972**, *72*, 315. − [6b] S. S. Krishnamurthy, A. C. Sau, M. Woods, *Adv. Inorg. Chem.* **1978**, *21*, 41.

[7] [7a] A. N. Chernega, M. Yu Antipin, Yu. T. Struchkov, I. E. Boldeskul, V. F. Shul′gin, V. D. Romanenko, *Zh. Strukt. Khim.* **1985**, *26*, 120. − [7b] V. D. Romanenko, V. F. Shul′kin, V. V. Skopenko, A. N. Chernega, M. Yu Antipin, Yu. T. Struchkov,

I. E. Boldeskul, L. N. Markovskii, *Zh. Obshch. Khim.* **1985**, *55*, 282. – [7c] M. Veith, M. Kross, J.-F. Labarre, *J. Mol. Struct.* **1991**, *248*, 345. – [7d] P. Braunstein, R. Hasselbring, D. Stalke, *New J. Chem.* **1996**, *20*, 337. – [7e] R. Hasselbring, H. W. Roesky, A. Heine, D. Stalke, G. M. Sheldrick, *Z. Naturforsch.* **1993**, *B48*, 43. For reviews on metal phosphazene complexes see: – [7f] M. Witt, H. W. Roesky, *Chem. Rev.* **1994**, *94*, 1163; [7g] H. R. Allcock, J. L. Desorcie, G. H. Riding, *Polyhedron* **1987**, *6*, 119.

[8] [8a] A. N. Chernega, M. Yu. Antipin, Yu. T. Struchkov, V. D. Romanenko, *Koord. Khim.* **1989**, *15*, 849. – [8b] S. K. Pandey, A. Steiner, H. W. Roesky, D. Stalke, *Inorg. Chem.* **1993**, *32*, 5444. – [8c] M. Krieger, R. O. Gould, K. Harms, S. Parsons, K. Dehnicke, *Chem. Ber.* **1996**, *129*, 1621. – [8d] D. Min, Y. Do, *Chem. Lett.* **1994,** 1989. – [8e] Y. Byun, D. Min, J. Do, H. Yun, Y. Do, *Inorg. Chem.* **1996**, *35*, 3981.

[9] [9a] S. K. Ray, R. A. Shaw, *J. Chem. Soc.* **1961**, 872. – [9b] V. Chandrasekhar, K. Vivekanandan, S. Nagendran, G. T. Senthil Andavan, N. R. Weathers, J. C. Yarbrough, A. W. Cordes, *Inorg. Chem.* **1998**, *37*, 6192.

[10] G. M. Sheldrick, *SHELX-97*, *X-ray structure determination programme*, Universität Göttingen, **1997**.

Received May 31, 1999
[I99189]